AUT Journal of Civil Engineering

AUT J. Civil Eng., 6(4) (2022) 447-460
DOI: 10.22060/ajce.2023.21848.5813

Numerical Evaluation of Unreinforced Masonry Brick Walls Retrofitted by Polypropylene Straps Subjected to Lateral Loading

K. Nasrollahzadeh[1]*, Sh. Ebrahimzadeh[2]

[1] Department of Civil Engineering, K. N. Toosi University of Technology, Tehran, Iran
[2] University of Southern Queensland, Centre for Future Materials, Toowoomba, Australia

ABSTRACT: This study investigated the two half-scale (1:2) unreinforced masonry walls, sharing identical dimensions, geometry, and construction characteristics, which were subjected to simultaneous lateral and vertical constant loading. While the first specimen represented an unreinforced masonry wall, the second specimen underwent a transformative retrofitting process involving the incorporation of vertical, horizontal, and oblique Polypropylene straps. To further optimize the retrofit, the minimum area of the wall was reinforced using shotcrete mortar with weak cement. The retrofitting material was defined by introducing Polypropylene straps and shotcrete mortar into the first model, and a comprehensive evaluation of the reference model was conducted. The pushover analysis, conducted through monotonic loading simulations, effectively replicated the essential behaviors observed in the primary experimental specimens. Remarkably, the experimental results exhibited striking agreement with the numerical outcomes derived from the employment of ABAQUS finite element software. Notably, these results unveiled the efficacy of the retrofitting technique, highlighting a remarkable enhancement in the ultimate lateral displacement by 140% and an impressive 71% increase in loading capacity. Furthermore, the retrofitting process induced a notable shift in the failure mode from diagonal tension and shear cracks to a more desirable flexural rocking mechanism, reinforcing the structural integrity of the masonry walls.

Review History:

Received: Oct. 12, 2022
Revised: Jun. 06, 2023
Accepted: Jul. 04, 2023
Available Online: Aug. 26, 2023

Keywords:

Numerical analysis
unreinforced masonry walls
retrofitting
polymeric straps
cyclic lateral loading

1- Introduction

Unreinforced masonry structures, both contemporary constructions and historic heritage buildings, are prevalent worldwide. However, these structures possess certain inherent limitations, such as moderate shear, compressive strength, and low tensile strength [1]. Due to the cyclic nature of earthquakes, unreinforced masonry walls must resist the combination of force actions, including shear forces, bending moments, vertical loads, and overturning moments [2]. This combination of loading actions, associated with the low tensile strength inherent in masonry, causes these structures vulnerable to inadequate seismic performance and heightened susceptibility to cyclic loading. This condition is more critical in Iran which has historically been struck by severe earthquakes (e.g., Bam on December 26, 2003, with 26000 people casualties) [3].

Laboratory experiments have revealed three main failure mechanisms in unreinforced masonry walls subjected to in-plane loading: shear cracking, bed-sliding, and flexural cracking (or rocking) [4]. However, the precise mechanism of lateral force resistance depends on several primary factors, which include the aspect ratio [5], boundary conditions [6], the magnitude of axial compression [2], and the characteristics of brick and mortar and their interface [7]. Understanding these factors is crucial for developing effective retrofitting strategies and improving the seismic performance of unreinforced masonry structures.

Seismic retrofitting of masonry buildings offers a range of options, varying from conventional steel ties and frames [5] to the application of welded wire mesh and plaster mortar layers on the walls [8]. In recent years, the use of polymeric fibers has gained popularity due to their non-corrosiveness, high strength-to-weight ratio, and reduced carbon emissions during manufacturing (e.g., GFRP sheets applied to the wall [9], the addition of polyvinyl alcohol fibers in the mortar [10], and the use of FRP strips [11]). However, the high cost of FRP materials and the skilled labor required for their application have led to an increased interest in utilizing polypropylene (PP) as a retrofitting material. PP has been successfully used to enhance the tensile strength of mortar [12] and as a grid mesh in the form of PP bands [13]. In recent years, an innovative approach for strengthening and repairing damaged unreinforced masonry walls using polypropylene (PP) bands and a minimal amount of cement-sand mortar [14]. This retrofitting method, which incorporates PP straps and weak cement mortar, has remarkably improved the seismic performance of unreinforced masonry walls.

The development of effective seismic improvement techniques for unreinforced masonry buildings necessitates numerical simulation that accurately captures the behavior of

*Corresponding author's email: nasrollahzadeh@kntu.ac.ir

(a) Unreinforced masonry wall (b) Retrofitted masonry wall

Fig. 1. Specimens in an experimental stage

these structures in both their un-strengthened and strengthened states. Numerical modeling of masonry seismic behavior has been approached in three main categories: macro modeling, detailed micro modeling, and simplified micro modeling [2, 15-16]. Micro-modeling involves separately representing each material component, such as bricks and mortar, using finite elements with zero-thickness interfaces to simulate their behavior. Non-linear constitutive laws are assigned to each material and interface, enabling a detailed analysis of their response. This approach provides a comprehensive understanding of mechanical behavior at the micro-level. On the other hand, macro modeling is suitable for studying large-scale masonry structures, focusing on the overall global behavior and response [17]. Simplified micro modeling, as the name suggests, simplifies the micro modeling approach, typically focusing on the finite element representation of mortar joints or zero-thickness interfaces between brick units. This approach offers a balance between accuracy and computational efficiency. While a significant portion of numerical modeling efforts has been dedicated to simulating the behavior of unreinforced masonry walls, fewer studies have focused specifically on modeling the performance of strengthening techniques. Therefore, further research and numerical modeling are necessary to explore and understand the behavior and effectiveness of various strengthening methods in detail.

This paper employs a numerical modeling approach based on simplified micro-modeling using concrete damage plasticity (CDP) to analyze the lateral load response of half-scale solid brick masonry walls. The study further investigates the impact of incorporating polypropylene (PP) bands and cement mortar plaster as a strengthening method. Through numerical modeling, the behavior of the strengthened walls is evaluated and compared with experimental results. The findings demonstrate a satisfactory agreement between the numerical predictions and the experimental observations. This numerical modeling strategy, utilizing simplified micro modeling and incorporating the strengthening technique, provides valuable insights into the lateral load response of masonry walls and the effectiveness of the applied strengthening method.

2- Experimental program

2- 1- Test setup and retrofitting method

The test specimens consisted of two half-scale unreinforced masonry specimens of dimensions 2000 × 1400 × 155 mm (length × height × width), respectively. While the former was an unreinforced masonry wall (Figure 1a), the latter was retrofitted by using a PP strap in horizontal, vertical, and oblique directions (Figure 1b). The PP straps are attached based on the crack pattern created in the first specimen test to prevent the spread of cracks. Regarding the material for retrofitting, it should be mentioned, Polypropylene fibres are widely used in industries related to the packaging and manufacture of plastic containers and have a low price. The retrofitted structure should be able to dissipate more energy and prevent the growth and propagation of the crack. To sentence this challenge, the strengthening technique must be employed and performed from the start of loading to achieve the best performance. For this purpose and to enclose the bands, a layer of cement-sand coating was applied on the surface of the wall with an average thickness of 20 mm.

In the experimental stage, both walls were subjected to cyclic quasi-static loading before and after the damage (Figure 2). The walls were tested by applying a constant vertical load of an average of 28 kN concurrently with a quasi-static reciprocating cyclic lateral load utilized by [5].

In each drift ratio, three reciprocating cycles are applied, then, half of the current amplitude is added, and three new cycles are performed to the sample. According to this loading protocol, the initial drift ratio of the protocol is equal to 0.2%, and the response interval of the fabricated specimens is linear.

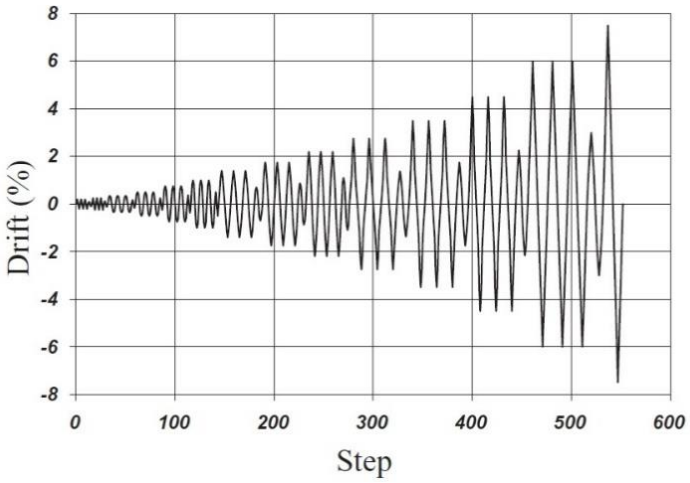

Fig. 2. Loading protocol [5]

However, based on the results of [14] the theoretical bi-linear equivalent force-displacement curve of the un-reinforced and retrofitted masonry walls has an acceptable agreement with experimental results. Hence, to save time in the process and simplicity it can investigate the pushover behavior of the samples in numerical modeling.

3- Analysis assumptions

The FE model was used to establish three-dimensional finite element models, in which the simplified micro-modeling approach was adopted for reproducing the behavior of the test walls, considering its acceptable computational costs and the capacity of reproducing the actual crack patterns of the masonry and comparison of push envelope of experiment and Finite Element analysis. The accurate representation of the three-phase environment in the reinforced sample, comprising masonry, polypropylene straps, and enclosing shotcrete mortar, is crucial for ensuring model convergence. The behavior of these materials plays a significant role in the modeling process. Once cracks form and the walls exhibit highly nonlinear and brittle characteristics, a dynamic explicit solver is employed as the numerical solving method.

The selection of a dynamic explicit solver is motivated by several factors. Firstly, as the model develops, a dynamic explicit solver proves to be more resource-efficient compared to a standard solver. This is particularly beneficial in handling larger and more complex models. Additionally, the dynamic explicit analysis does not require an assembly matrix, making it well-suited for solving intricate contact problems. Moreover, it offers advantages over static general analysis in terms of solving complex contact interactions [18].

4- Material characteristics

For the designation of the material behavior, the mechanical properties of the construction materials i.e., brick, cement-sand mortar, and PP bands were tested in the experimental stage (Table 1).

4- 1- PP-band

In the numerical modeling, due to the higher width of the PP straps compared to their thickness, a shell element with a mesh size (S4R) of 20 mm was utilized to represent the Polypropylene (PP) bands. The behavior of the PP bands was characterized using a linear elastic model, as determined from material tests conducted by [14]. The linear elastic model assumes that no plastic strain occurs in the post-cracking range, ensuring that the stress-strain curve's unloading paths always pass through the origin of the coordinate system. The model adopts Young's modulus of 2 GPa (average of the punched and without punched), obtained from the conducted material tests (Table 1). Additionally, a Poisson's ratio of 0.2 was applied to the model, further characterizing the PP bands' mechanical response.

4- 2- Plaster mortar

To represent the plaster mortar on both sides of the wall surface, planar shell elements with an S4R mesh type and a mesh size of 20 mm were employed. The elastic behavior of the mortar was characterized by Young's modulus of 1850 MPa and a Poisson's ratio of 0.2. To capture the nonlinear behavior of the mortar, including cracking and crushing, the concrete damaged plasticity (CDP) model proposed by [19] was utilized. The plasticity parameters were adopted from the study conducted by [20]. Additionally, a viscosity parameter value of 0.0005, derived from [21], was implemented in the analysis. A sensitivity analysis was conducted to evaluate the impact of this parameter on the results. Comparisons between the default value (0) in ABAQUS and the specific value used in the explicit dynamic analysis indicated slight differences in the outcomes. It is noteworthy that the compressive and tensile parameters, such as yield stress, inelastic strain, and cracking strain, had a significant influence on the model's performance

Table 1. Mechanical properties of materials [14]

Parameter	Numerical value
Cement-sand ratio	1:6
Compressive strength (MPa)	~ 4.1
Shear Strength from In-situ shear test (MPa)	~ 1
Mean shear strength of the mortar from the uniaxial test (MPa)	0.09
Compressive strength of the brick (MPa)	5.7
Modulus of elasticity (MPa)	1084
Tensile strength of the PP-band (MPa)	133.3
Elastic modulus of the PP-band (GPa)	3.7
Tensile strength of the PP-band with punched clips (MPa)	70.62
Elastic modulus of the PP-band with punched clips (GPa)	2.01

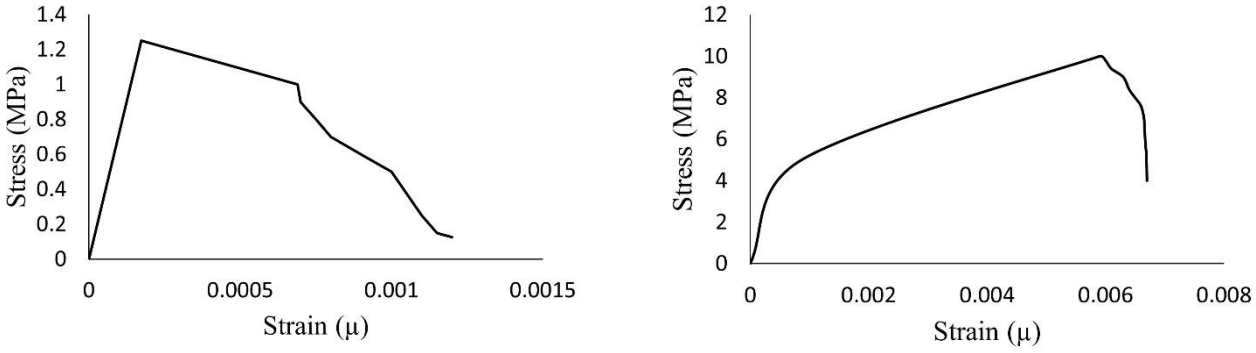

(a) Tension behavior (b) Compression behavior

Fig. 3. Stress-strain behavior of mortar

(Table 2). The tensile and compressive behavior of the mortar has been demonstrated based on the experimental results [14].

The concrete-damaged plasticity (CDP) model employed in this study captures the nonlinear behavior of mortar by establishing relationships between various parameters. These parameters include inelastic strain (ε_c^{in}), plastic strain (ε_c^{pl}), mortar compression strength (σ_c), and damage parameter (d_c). The compressive behavior of concrete in this study follows the model proposed by [22]. The stress-strain relationship is defined by the following equations:

$$\sigma_c = \left(\frac{\beta\left(\frac{\varepsilon_c}{\varepsilon_0}\right)}{\beta - 1 + \left(\frac{\varepsilon_c}{\varepsilon_0}\right)^{\beta}}\right)\sigma_{cu} \quad (1)$$

Table 2. Designated parameters of CDP for mortar

Properties							
General properties		**Plasticity properties**		**Compressive behavior**		**Tensile behavior**	
Density (Ton/mm^3)	2.4-09	Dilation angle (ψ)	35	Yield stress (MPa)	Inelastic strain	Yield stress (MPa)	Cracking stain
Young modulus (MPa)	1850	Eccentricity	0.1	2.5	0	1.25	0
				5	0.000494595	1	0.000170519
				4.9	0.000702703	0.9	0.000232468
				4.7	0.001018919	0.8	0.000334416
				4.5	0.001435135	0.7	0.000436364
				4.2	0.001859459	0.6	0.000588312
				4	0.002175676	0.5	0.00074026
				3.8	0.002491892	0.25	0.00097013
				3.5	0.002866216	0.15	0.001072078
				3.2	0.003200541	0.125	0.001135065
				3	0.003426757		
				2.8	0.003652973		
				2.6	0.003879189		
				2	0.004537838		
Poisson's ratio	0.2	f_{b0}/f_{c0}	1.12				
		K_c	0.6667				
		Viscosity	0.0005				

$$\beta = \frac{1}{1-[\sigma_{cu}-(\varepsilon_0 E_0)]} \quad (2)$$

$$\varepsilon_0 = 8.9\times10^{-5}\sigma_{cu} + 3.28312\times10^{3} \quad (3)$$

The concrete damage parameter for compression was determined based on $(1-(\frac{\sigma_c}{\sigma_{co}}))$, while the value for tension was based on $(1-(\frac{\sigma_t}{\sigma_{t0}}))$ from the model of [22]. In the mentioned equations for the damage parameter (σ_{cu}) and (σ_{t0}) are the maximum compressive and tensile strength achieved in the material test. The values of the model for the plaster cement mortar were provided (Table 2).

4- 3- Masonry unit (brick and mortar)

To represent the behavior of the mortar and brick, solid elements with a C3D8R meshing type and a size of 10 mm were employed as designated in other studies [20, 23]. However, to simplify the modeling process and enhance computational efficiency, a simplified micro-model strategy was adopted. This strategy involved treating the mortar and brick as an equivalent masonry unit. For the masonry unit, Young's Modulus, maximum compressive strength, and tensile strength were determined to be 3850 MPa, 10 MPa, and 2.5 MPa, respectively. It should be noted that the calculation of the concrete-damaged plasticity (CDP) parameters for the masonry unit followed the same approach as that for the mortar, as outlined in Table 3.

To construct the model, elements were assembled based on the physical construction of the unreinforced masonry wall (Figure 4a). Subsequently, the retrofitted parts were added to the model to simulate the strengthened configuration (Figure 4b). This modeling approach allowed for the representation of the structural components and their interaction, enabling the analysis of the behavior of both the original and retrofitted masonry walls.

5- Element interface and loading

The interaction between the elements in the numerical model was defined based on tangential and normal interactions. The tangential interaction was represented by a friction coefficient of 1, while the normal interaction was

Table 3. Designated parameters of CDP for masonry unit

Properties							
General properties		**Plasticity properties**		**Compressive behavior**		**Tensile behavior**	
Density (Ton/mm^3)	1.9-09	Dilation angle (ψ)	35	Yield stress (MPa)	Inelastic strain	Yield stress (MPa)	Cracking stain
Young modulus (MPa)	3850	Eccentricity	0.1	5	0	2.5	0
				10	0.003302597	2	0.000170519
				9.8	0.003454545	1.8	0.000232468
				9.4	0.003658442	1.6	0.000334416
				9	0.003962338	1.4	0.000436364
				8.4	0.004218182	1.2	0.000588312
				8	0.004422078	1	0.00074026
				7.6	0.004625974	0.5	0.00097013
				7	0.004831818	0.3	0.001072078
				6.4	0.004997662	0.25	0.001135065
				6	0.005111558		
				5.6	0.005225455		
				5.2	0.005339351		
				4	0.005661039		
Poisson's ratio	0.15	f_{b0}/f_{c0}	1.12				
		K_c	0.6667				
		Viscosity	0.0005				

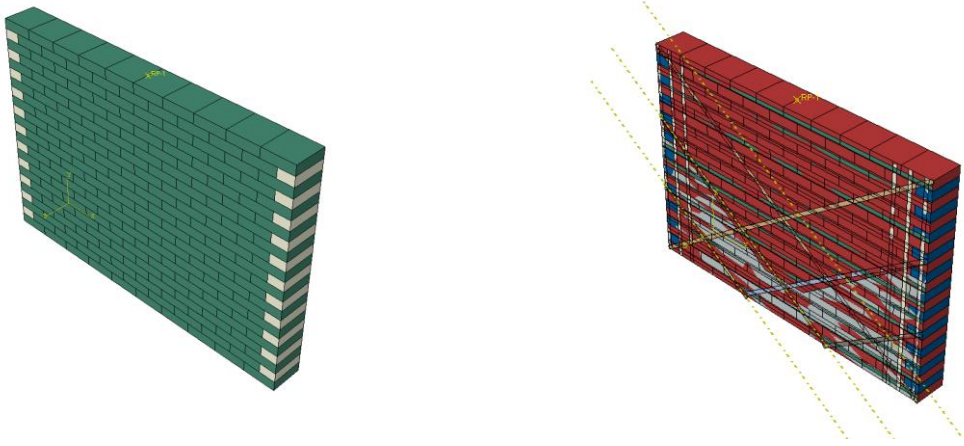

(a) Unreinforced masonry wall (b) Retrofitted specimen

Fig. 4. General view of the constructed FEM model

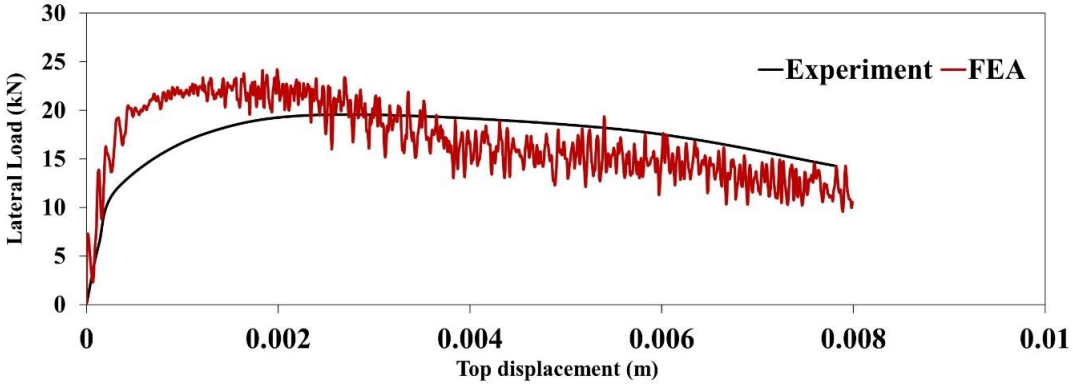

(a) Unreinforced masonry wall

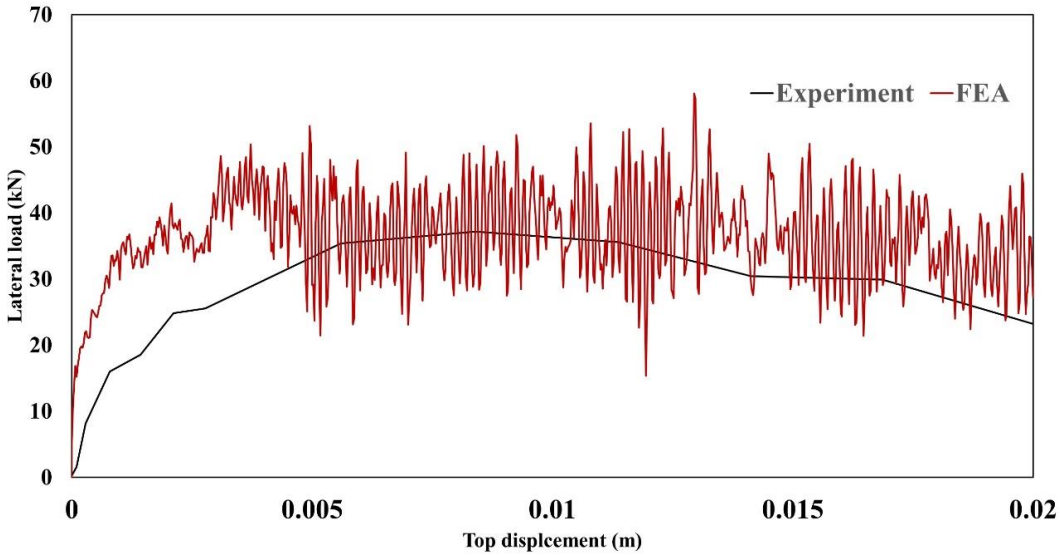

(b) Retrofitted masonry wall

Fig. 5. Lateral load-displacement curves of the experimental result and numerical modeling

modelled as a hard contact [20]. To simulate the experimental conditions accurately, a constant compressive axial load of 14.7 kN, corresponding to the experimental program, was applied to the masonry wall in the numerical model. The pushover behavior of the wall was investigated by subjecting the specimen to a lateral displacement of 25mm. Since the polypropylene (PP) band provides confinement to the wall and remains attached to the specimen throughout the test, the interface between the PP band and the wall was simulated using a constraint known as a "Tie" constraint. This constraint ensures that the elements representing the PP band and the wall remain connected throughout the analysis, accurately representing their interaction.

6- Result and discussion

6- 1- Load capacity behavior

The load-displacement curves obtained from the monotonic finite element model analyses and backbone curves resulting from the experimental tests are compared and there is a good agreement between the experimental and numerical results (Figure 5). The behavior of both the unreinforced and retrofitted masonry walls can be divided into two stages. The first stage is the pre-crack phase, during which both the unreinforced and retrofitted specimens exhibit linear elastic behavior. In this stage, the specimens respond linearly to the applied loads. Once cracks start to form and propagate, the second stage, known as the post-crack stage

or the nonlinear stage, is initiated. In this stage, the behavior of the masonry walls becomes nonlinear, characterized by crack development and the redistribution of stresses. It is worth mentioning that in the post-crack stage, the retrofitted specimen demonstrates improved performance compared to the unreinforced specimen. On average, the retrofitted specimen exhibits a maximum lateral bearing capacity that is approximately 13% higher than the ultimate strength observed in the tested sample. This indicates the effectiveness of the retrofitting method in enhancing the structural strength and load-bearing capacity of the masonry walls.

An overestimation of the numerical analysis happened in the pre-crack and post-crack stages for both models. This behavior in unreinforced masonry walls (model 1) may attribute to the lower strength of the cement-sand mortar applied in the wall construction which caused the initiation of the first crack to happen earlier than predicted. Moreover, due to the simplified- micro approach for the modeling instead of the brick and mortar, equivalent brick with a material behavior constructed from concrete damaged plasticity, representing brick and mortar. This equivalency caused simplicity and saved time, however, the friction coefficient between the equivalent brick in the bed joint in the model is higher than it's the real one, causing a higher cracking lateral loading. With the development of the crack (2.5 mm) and losing the friction between the elements, the behavior became closer to the experimental specimen and the results of the finite element model of unreinforced specimens after lateral drift of 0.2% match the results very well.

In contrast, the over-estimation in the retrofitted wall (model 2) continued from the beginning of the loading which may be attributed to the above reason in the pre-crack stage. However, in the post-crack stage (from 2.5mm to 5.5 mm) which is associated with non-linear behavior and represents a widening of the cracks, the PP straps in the experimental specimen acted with a little bit of delay. This is due to the hand-tightening of the straps and justified the reason for the application of the mortar in the wall surface for more enclosing the PP straps.

6- 2- Failure mechanism behavior

The joint bed sliding and diagonal tension cracks in the unreinforced have a similar propagation pattern (Figures 6a-b). The failure mode of the unreinforced masonry wall specimen started with the first crack and the spread of the diagonal-tensile crack pattern. Also, the diagonal cracks were formed due to the connection of vertical and horizontal cracks that appeared at the height of one-third of the bottom of the wall. The failure mode of the specimen was considered as a mixing of the two main in-plane modes observed in the specimens which is the combination of the shear-slip and diagonal failure modes.

In the toe regions, the stress is more than on other parts of an unreinforced masonry wall (Figure 6c). Since the analysis was performed in monotonic loading, it could be deduced that the other toe section of the wall may have this phenomenon. The failure mode of the strengthened specimen was rocking motion. A crack was created in the toe of the wall and a layer of cement-sand coating caused a spalling and separation of the coating from the specimen surface. Additionally, the retrofitting technique has effectively enhanced the behavior of the strengthened wall, leading to the stress being transferred to the polypropylene (PP) straps. This can be observed in Figure 7a, where the principal stress in the shotcrete mortar and PP straps at the corners of the walls results in a rocking behavior. Consequently, the propagation of damage concentrates in the toe region, as depicted in Figure 7b.

7- Effect of the retrofit

The initial stiffness of the masonry walls subjected to lateral loading is calculated in the linear-elastic stage. To do that, the initial stiffness, K_i, is defined as the slope of the experimental envelope curve at the origin to a drift of 0.1 % (Table 4) [5]. Retrofitting method affects the ductility parameters in both linear-elastic (160% improvement) and post-crack stages by (140%) increasing the capacity for higher displacement. By retrofitting the wall, the bearing capacity in the pre-crack (86% enhancement) and ultimate stage (71%) improved, however, due to the increase in the ductility, the initial stiffness of the wall decreases compared to the unreinforced state. Increased ductility has led to an increase in the energy dissipation capacity of the specimens, which is of importance for unreinforced masonry walls.

8- Parametric study

8- 1- Mortar properties

The retrofit method, which involves the presence of both mortar and a polypropylene (PP) band, was primarily focused on evaluating the effectiveness of the PP band while disregarding the contribution of the low-strength mortar in providing confinement. This section aims to investigate the influence of the mortar and assess the validity of this assumption in the retrofitting method.

To explore the effect of the mortar, the ultimate compressive strength of the mortar was assumed to be twice as high at 10 MPa (Figure 8). Since the material test only examined the concrete's compressive strength, the mortar's ultimate tensile strength was estimated using Equation 4 [24].

$$\sigma_{t0} = 0.33\sqrt{\sigma_{cu}} \quad (4)$$

As anticipated, by improving the properties of the mortar (100% enhancement), the cracking load increased just by 20%. However, it was observed that after the formation of cracks and the initiation of the non-linear stage, the ultimate lateral load capacity remained unchanged. This can be attributed to the higher contribution of the PP band in enhancing the retrofitting method. The effect of the weak mortar on the wall surface can be summarized as providing pure confinement for the PP band, ensuring that their effectiveness is not delayed.

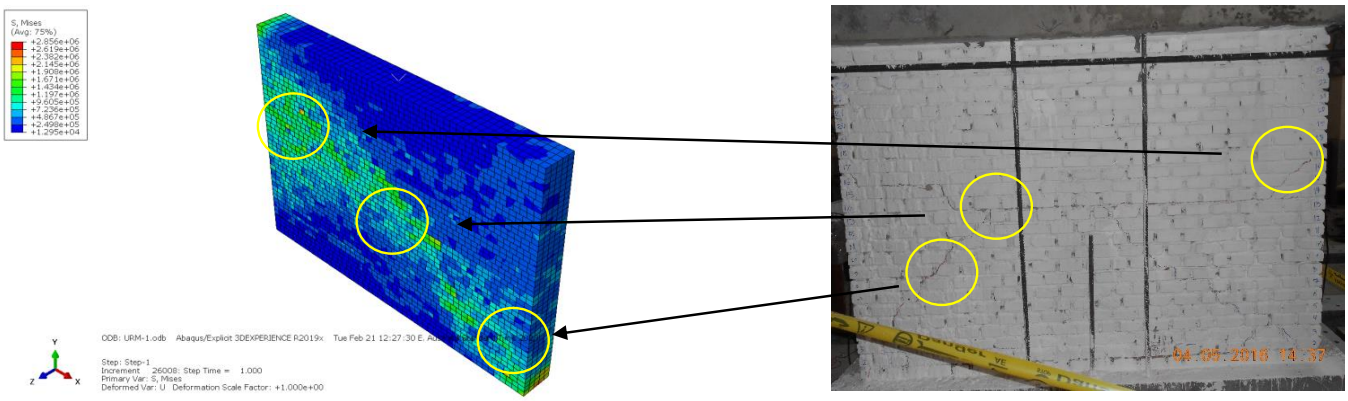

(a) URM (FEM) (b) URM (Experiment)

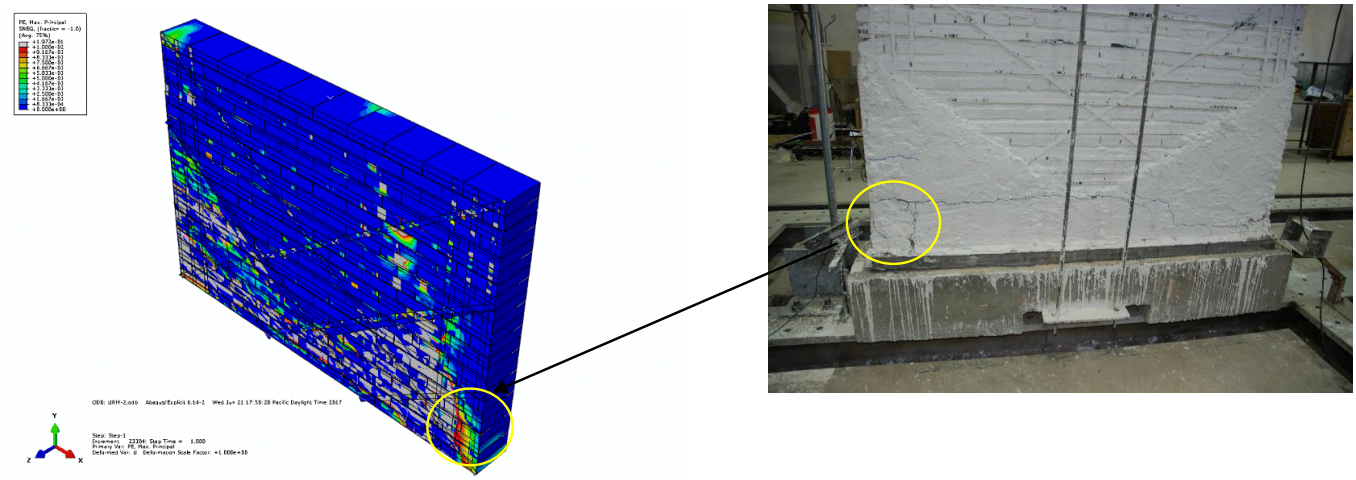

(c) Retrofitted (FEM) (d) Retrofitted (Experiment)

Fig. 6. The failure mechanism of the masonry walls

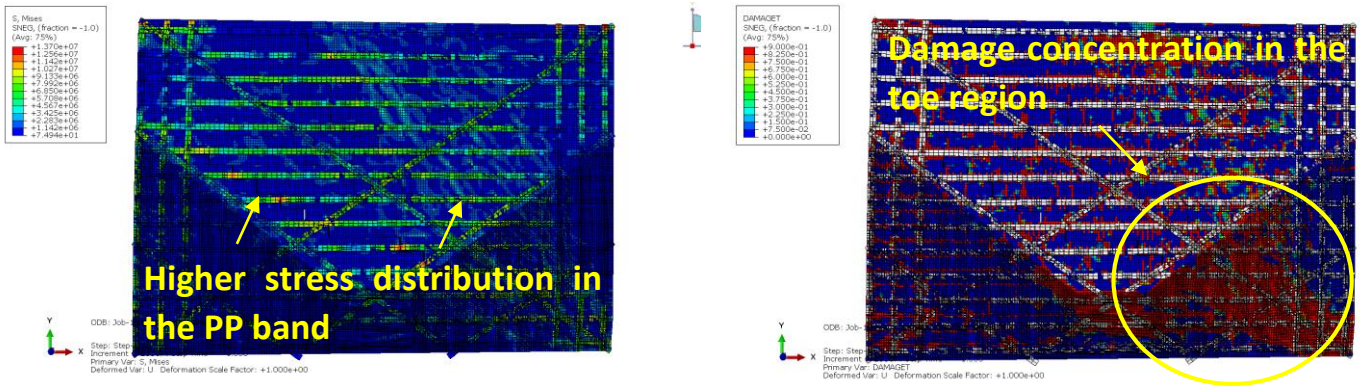

(a) Stress distribution (b) Damage propagation

Fig. 7. Failure behavior of the retrofitted masonry wall

Table 4. The results of the idealization of specimens.

Specimens' stiffness and ductility parameters						
	Lateral stiffness	Elastic stage		Ultimate stage		Ductility
	Initial stiffness K_i (kN/mm)	Lateral load V_y (kN)	Elastic Displacement d_e (mm)	Lateral load V_u (kN)	Displacement d_u (mm)	$\mu = d_u / d_e$
Unreinforced masonry wall						
Average	17.3	10.4	0.6	21	7.7	12.83
PP-retrofitted masonry wall						
Average	16.1	19.4	1.6	36	18.5	11.6

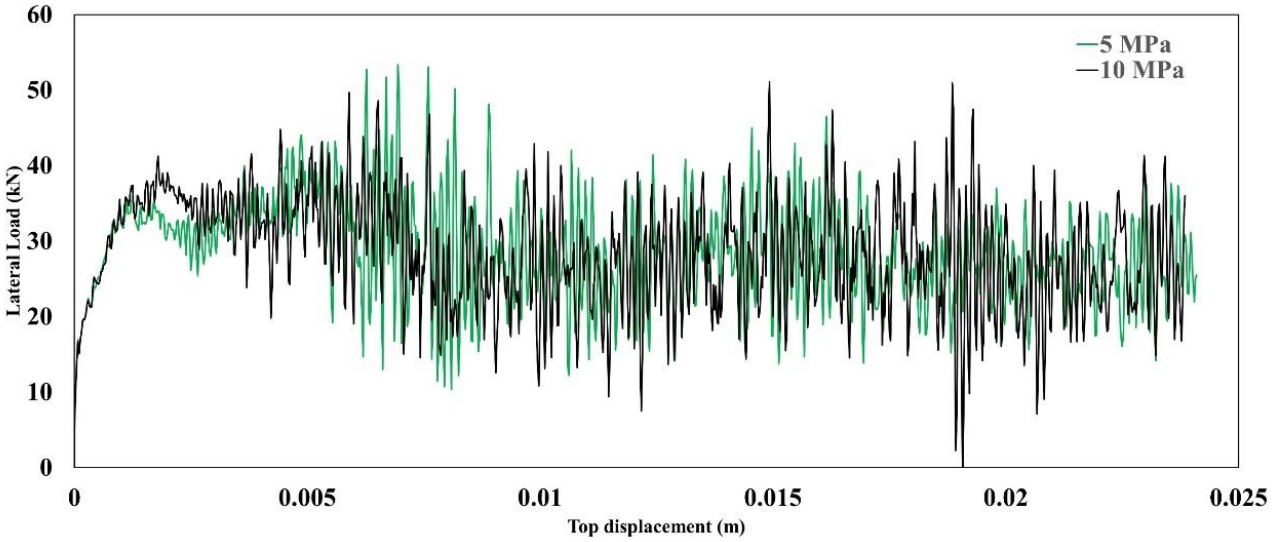

Fig. 8. Impact of the mortar strength

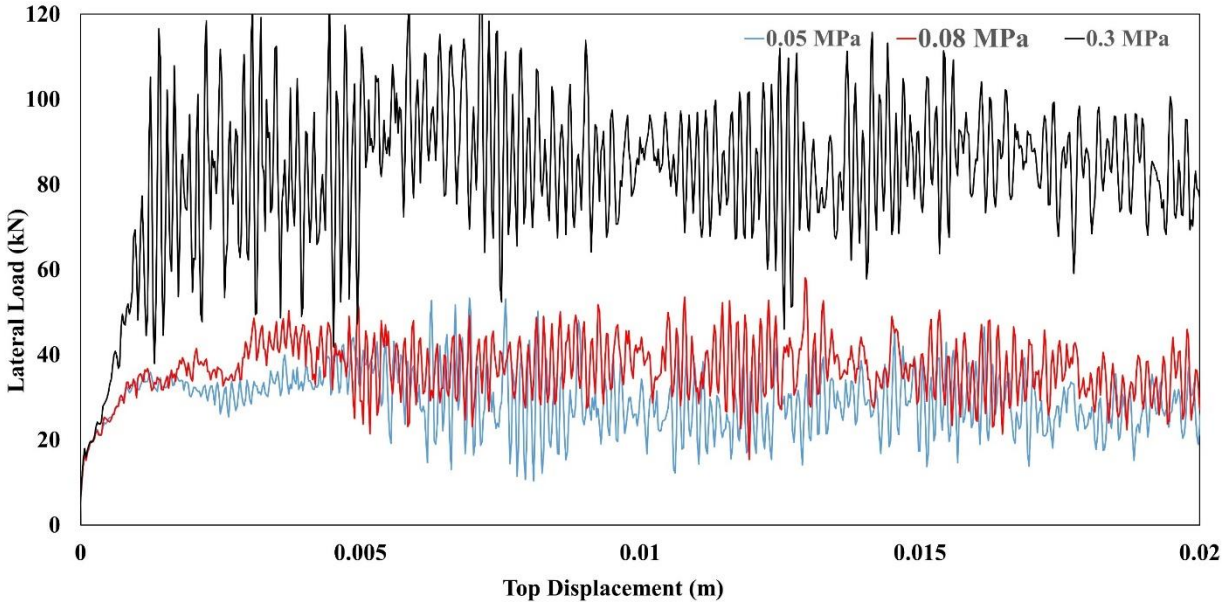

Fig. 9. Impact of the compression stress

8- 2- Axial compressive stress

In the parametric study, the effect of the level of constant axial stress on the retrofitted masonry wall was investigated. Three levels of axial stress were considered: 14.7 kN (0.05 MPa), 24.5 kN (0.08 MPa), and 98 kN (0.3 MPa) (Figure 9). As expected, increasing the level of axial stress increased the ultimate strength of the retrofitted wall, which is consistent with the findings of [2]. However, when comparing the two lower levels of compression stress (0.05 and 0.08 MPa), there were no significant changes observed in the initial stiffness and lateral load capacity of the retrofitted wall. In contrast, the higher axial stress level (0.3 MPa) showed notable effects. Based on these results, it is suggested that a minimum pre-compression level of 0.1 MPa, as proposed in other studies [2, 25], is necessary to achieve significant improvements in the unreinforced and retrofitted wall's behavior.

9- Conclusion

In this paper, the seismic behavior of masonry walls strengthened and un-strengthened with polypropylene bands and weak cement mortar shotcrete was evaluated through finite element analyses. The results of both the experimental study

and the numerical model for the stress distribution and lateral displacement contour are noted to be in good agreement. The significant conclusions and main contributions of this study are as followings:

The proposed retrofitting method increased the ductility index in pre- and post-crack stages by 160 and 140% respectively. Furthermore, load capacity in the linear elastic and non-linear stages is enhanced by 86 and 71% respectively.

The retrofitting method caused the change in failure mode from a combination of the shear and diagonal tension to the rocking mode and it's in agreement with the FEA results.

The concrete damage plasticity (CDP) model was able to accurately predict the nonlinear and post-cracking behavior of the unreinforced and retrofitted masonry wall. The retrofitted model was found to be particularly more sensitive to the presence of the PP band than the tensile behavior of the mortar.

It is observed that the level of pre-compression below 0.1 MPa does not significantly affect the pre-crack behavior and initial stiffness of the retrofitted wall. In this interval, the changes in pre-compression do not have a noticeable impact. However, when the stress level exceeds 0.1 MPa and reaches 0.3 MPa, there is an increase in both the initial stiffness and ultimate load capacity of the retrofitted wall. This indicates that beyond the threshold of 0.1 MPa, the level of pre-compression plays a more significant role in improving the structural performance of the retrofitted wall.

References

[1] Shabdin, M., Nader KA Attari, and M. Zargaran. "Shaking table study on the seismic performance of an Iranian traditional Un-Reinforced Masonry (URM) building." In Structures, Elsevier, (27) (2020) 424-439.

[2] Vemuri, Jayaprakash, Syed Ehteshamuddin, and Subramaniam Kolluru. "Numerical simulation of soft brick unreinforced masonry walls subjected to lateral loads." Cogent Engineering, 5(1) (2018) 1551503.

[3] Ahari, Gholamreza ZAMANI, and Kentaro Yamaguchi. "A proposal of the most suitable retrofitting methods for URM structures in Iran. An extensive review of recent techniques." Journal of Habitat Engineering, (2) (2010) 105-114.

[4] Tomazevic, Miha. Earthquake-resistant design of masonry buildings. Vol. 1. World Scientific, 1999.

[5] Darbhanzi, A., M. S. Marefat, and M. Khanmohammadi. "Investigation of in-plane seismic retrofit of unreinforced masonry walls by means of vertical steel ties." Construction and Building Materials, (52) (2014) 122-129.

[6] Haach, Vladimir G., Graça Vasconcelos, and Paulo B. Lourenço. "Parametrical study of masonry walls subjected to in-plane loading through numerical modeling." Engineering Structures, 33(4) (2011) 1377-1389.

[7] Petrovčič, Simon, and Vojko Kilar. "Seismic failure mode interaction for the equivalent frame modeling of unreinforced masonry structures." Engineering structures, (54) (2013) 9-22.

[8] Padalu, Pravin Kumar Venkat Rao, Yogendra Singh, and Sreekanta Das. "Cyclic two-way out-of-plane testing of unreinforced masonry walls retrofitted using composite materials." Construction and Building Materials, (238) (2020) 117784.

[9] Mahmood, Hamid, A. P. Russell, and J. M. Ingham. "Laboratory testing of unreinforced masonry walls retrofitted with glass FRP sheets." In Proceedings of the 14th International Brick/Block Masonry Conference, Sydney, Australia, (1720) (2008).

[10] Deng, Mingke, and Shuo Yang. "Cyclic testing of unreinforced masonry walls retrofitted with engineered cementitious composites." Construction and Building Materials, (177) (2018) 395-408.

[11] Chuang, Shih-Wei, Y. Zhuge, T. Y. Wong, and L. Peters. "Seismic Retrofitting of Unreinforced Masonry Walls by Frp Strip." PhD diss., New Zealand Society for Earthquake Engineering, (2003).

[12] Mustafaraj, Enea, and Yavuz Yardim. "Retrofitting damaged unreinforced masonry using external shear strengthening techniques." Journal of Building Engineering, (26) (2019) 100913.

[13] Dutta, Sekhar Chandra, Parthasarathi Mukhopadhyay, and Kundan Goswami. "Augmenting strength of collapsed unreinforced masonry junctions: Principal damage feature of walls damaged by moderate indian earthquakes." Natural Hazards Review, 14(4) (2013) 281-285.

[14] Ebrahimzadeh, Shahrad, and Kourosh Nasrollahzadeh. "Experimental study on performance of repaired and strengthened unreinforced masonry walls using polypropylene bands." Scientia Iranica (2022).

[15] Farahani, Emadoddin Majdabadi, Mohammad Yekrangnia, Masoud Rezaie, and Rita Bento. "Seismic behavior of masonry walls retrofitted by centercore technique: A numerical study." Construction and Building Materials, 267 (2021) 120382.

[16] Vera, Mónica Y. Oña, Giovanni Metelli, Joaquim AO Barros, and Giovanni Plizzari. "New openings in unreinforced masonry walls under in-plane loads: a numerical and experimental study." International Journal of Masonry Research and Innovation, 6(2) (2021) 166-195.

[17] Abdulla, Kurdo F., Lee S. Cunningham, and Martin Gillie. "Simulating masonry wall behavior using a simplified micro-model approach." Engineering Structures, (151) (2017) 349-365.

[18] Su, Zhiming, Wenzhong Zheng, Ying Wang, and Xiaomeng Hou. "Seismic Vulnerability Analysis of Masonry Structures Built with Disassembled Brick Wall Sections." Buildings, 12(11) (2022) 1831.

[19] Lubliner, Jacob, Javier Oliver, Sand Oller, and EJIJos Onate. "A plastic-damage model for concrete." International Journal of solids and structures, 25(3) (1989) 299-326.

[20] Bolhassani, Mohammad, Ahmad A. Hamid, Alan CW Lau, and Franklin Moon. "Simplified micro modeling of partially grouted masonry assemblages." Construction and Building Materials, (83) (2015) 159-173.

[21] Demir, Aydin, Hakan Ozturk, Kemal Edip, Marta Stojmanovska, A. Bogdanovic, and E. Seismology. "Effect of viscosity parameter on the numerical simulation of reinforced concrete deep beam behavior." The Online Journal of Science and Technology, 8(3) (2018) 50-56.

[22] Hsu, L. S., and C-TT Hsu. "Complete stress—strain behavior of high-strength concrete under compression." Magazine of concrete research, 46(169) (1994) 301-312.

[23] Deng, Mingke, and Shuo Yang. "Experimental and numerical evaluation of confined masonry walls retrofitted with engineered cementitious composites." Engineering Structures, (207) (2020) 110249.

[24] Genikomsou, Aikaterini S., and Maria Anna Polak. "Finite element analysis of punching shear of concrete slabs using damaged plasticity model in ABAQUS." Engineering structures, (98) (2015) 38-48.

[25] Zeng, Bowen, Yong Li, and Carlos Cruz Noguez. "Modeling and parameter importance investigation for simulating in-plane and out-of-plane behaviors of unreinforced masonry walls." Engineering Structures (248) (2021) 113233.

HOW TO CITE THIS ARTICLE

K. Nasrollahzadeh, Sh. Ebrahimzadeh, Numerical Evaluation of Unreinforced Masonry Brick Walls Retrofitted by Polypropylene Straps Subjected to Lateral Loading, AUT J. Civil Eng., 6(4) (2022) 447-460.

DOI: 10.22060/ajce.2023.21848.5813